

Local order in a dense liquid

H. J. M. Hanley,* T. R. Welberry, D. J. Evans, and G. P. Morriss

Research School of Chemistry, Australian National University, G.P.O. Box 4, Canberra, Australian Capital Territory 2601, Australia

(Received 7 December 1987)

Transient local hexagonal order in a dense liquid is observed in a molecular-dynamics simulation of two-dimensional soft disks. Instantaneous local structure factors at a particular density are obtained using an optical transform of the particle coordinates for a single configuration. Local hexagonal order is quantified using an order parameter, and its lifetime characterized by the decay of the order-parameter autocorrelation function. This type of transient structure is significant at densities greater than $\frac{7}{10}$ of the freezing density, and becomes persistent near the freezing density.

INTRODUCTION

In this paper we demonstrate a transient local ordered structure in a dense liquid. While it has long been recognized that local anisotropic ordering must be present in a fluid—the change of the typical isotropic liquid microstructure to that of the anisotropic solid, and the converse, has been studied extensively in the context of crystal growth, supercooling, and glass formation^{1–6}—our work differs in that the simulated fluid is probed *in situ* as an equilibrium liquid at constant temperature and density.

Our conclusions are based on the local structure factor and an order parameter evaluated from the standard “SLOD” molecular-dynamics simulation of a two-dimensional fluid. Details of the technique have been reported elsewhere,⁷ and previous simulations of the two-dimensional liquid have been discussed at length by us and by others.⁸ In this work the systems consisted of 3584 or 896 soft-disk particles interacting with an inverse-twelfth-power potential truncated and shifted at $r = 1.5$. Simulations were carried out with the system at constant density ρ , and kinetic temperature T , for a given state point, $X = \rho T^{-1/6}$ with the temperature constrained at 1.0. (All variables are reduced by the potential parameters that are in turn set equal to one, as is the usual practice.) The results presented here were extracted from simulation runs of approximately 20 000 time steps, with the time step equal to 0.004, for liquid densities in the range $0.3 \leq \rho \leq 0.98$, and for one density in the solid at $\rho = 1.05$. The freezing density for an 896 particle system has been determined previously⁹ to be 0.986 ± 0.001 . We made sure the system was properly equilibrated at zero time.

LOCAL STRUCTURE FACTOR

The presence of anisotropic local order in an individual snapshot of the simulation was first detected when we made use of an optical transform method¹⁰ of probing the structure factor $S(\mathbf{k})$. We had previously used this optical method in a nonequilibrium molecular-dynamics (NEMD) study of shear-induced anisotropy in two-dimensional liquids.¹¹ Initially the method was used to parallel some published diffraction work on a real colloidal system, but it proved such a simple and effective way of monitoring $S(\mathbf{k})$ that we continued to use it, in preference to an earlier method¹² involving the Fourier

transforming of the spherical harmonic expansion of the pair correlation function.

Optical transform methods are well established as aids to the interpretation of diffraction phenomena in the solid state, but their use in conjunction with MD simulation of liquids is quite novel so we give a brief description of the procedure. To evaluate the structure factor $S(\mathbf{k})$ we extracted the positions of the particles from the simulation run at a particular time. The key step was to represent these positions as transparent dots on otherwise black photographic film. We scaled the simulation cell length to 16.6 mm on the film and a particle coordinate was represented by a 200 μm diameter dot. It should be remarked that the actual size of the dot affects only the overall variation of scattered intensity with diffraction angle, not the structure factor itself. The structure factor followed as a direct measurement simply by taking the film as a scattering medium and obtaining a diffraction pattern using light from a low power He-Ne laser.^{10,11} For the 896-particle liquid, composite plots were prepared that consisted of thirty-six data sets taken at random times from the appropriate simulation. The sets were arranged side by side on a 6×6 grid covering an area of $10 \text{ cm} \times 10 \text{ cm}$ on the film. Since there can be virtually no phase coherence between light scattered from the separate plots, the resulting intensity is the average of the individual transforms. The position of the particles on each plot was estimated to be accurate to 0.04%. One plot was prepared for the 3584-particle system at a density 0.9238, scaling the dot size and interparticle distance to be consistent with the smaller system. The structure factors from this sample were extracted by viewing the sample as a whole, and by stopping down the aperture to look at smaller segments of about 800 particles.

Structure factors for the 896-particle system are presented in Fig. 1. Figure 1(a) depicts the hexagonal crystalline pattern of the solid at $\rho = 1.05$; Fig. 1(b) was constructed for the system at a density of 0.95 and shows the typical circularly symmetric pattern of a dense liquid; Fig. 1(c) shows the diffuse structure of the moderately dense liquid at $\rho = 0.3$. As remarked, these intensity plots are averages of thirty-six configurations taken at random times. A more detailed picture emerges when the structure factor is evaluated from an individual configuration. For example, Fig. 2 displays *snapshots* of $S(\mathbf{k})$ from the run at $\rho = 0.95$; Fig. 2(a) shows the pattern

expected for a liquid, but Fig. 2(b) taken from the simulation 50 time steps later, indicates anisotropic features reminiscent of the microstructure of the solid. In particular, the second diffuse ring in Fig. 2(b) appears hexagonal in shape while in the inner ring there are six spots of rather brighter intensity. These two examples were chosen from a set of 36 snapshots taken at regular intervals during the simulation. In approximately half of the snapshots this hexagonal structure was clearly evident, although the orientation of the hexagonal structure varied.

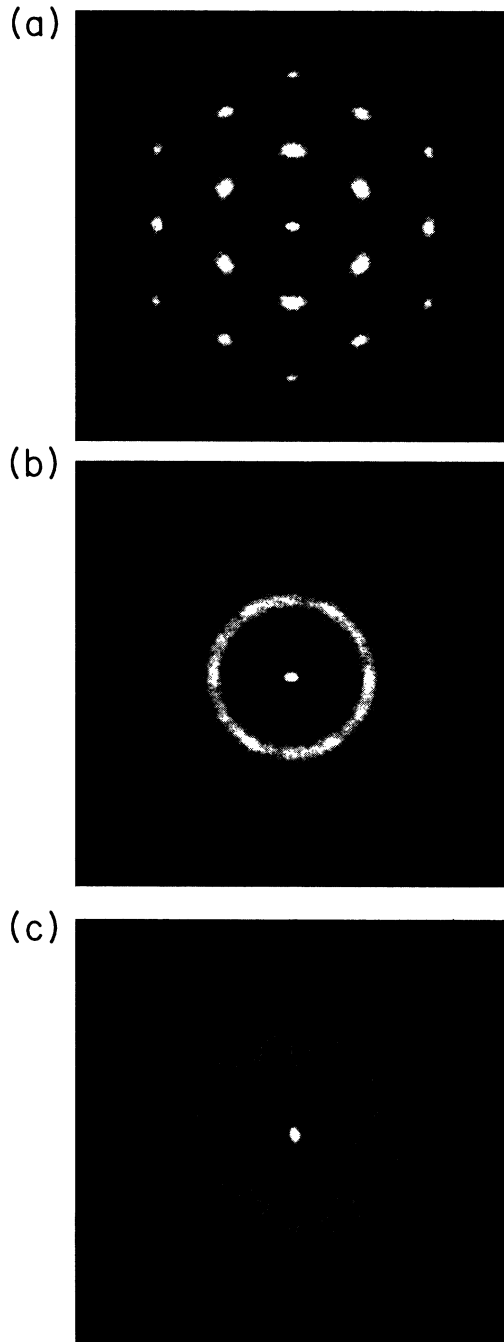


FIG. 1. Average structure factors for the 896-particle soft-disk system at three densities. (a) The solid at $\rho=1.05$; (b) dense liquid at $\rho=0.95$; (c) the liquid at $\rho=0.3$.

The information contained in Fig. 2 can also be displayed in r space. For each particle in a configuration we construct a bond vector by joining its center to the center of its nearest neighbor. Taking the midpoint of the bond as the origin, and its direction as a reference angle we plotted the positions of its near neighbors. The results in Figs. 3(a) and 3(b) correspond to the configurations used to obtain Figs. 2(a) and 2(b), respectively. Visual evidence of hexagonal order is clear in Fig. 3(b) in both the first- and second-neighbor shells.

The structure factor for the liquid with 3584 particles at $\rho=0.9238$ is shown as Fig. 4. Figure 4(a) is the resultant $S(\mathbf{k})$ for the whole sample, i.e., obtained by exposing the total area to the light beam, while Figs. (b) and (c) were obtained from segments of the sample. Again we see evidence of the hexagonal order, but observed as a function of sample area rather than of time as in Figs. 2 and 3.

ORDER PARAMETER

The degree of hexagonal order as a function of density was correlated in terms of a conveniently chosen order parameter ξ , defined as $\langle \cos 6\phi \rangle$, where ϕ is the orientation angle between a particle and its neighbor found in the ring of thickness dr , distance r away. With reference

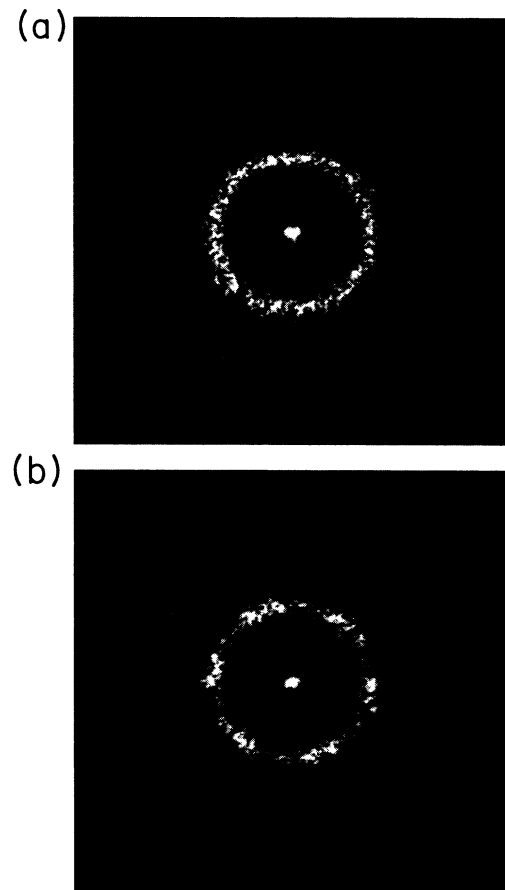


FIG. 2. The structure factor for the liquid at $\rho=0.95$ evaluated from the simulation at two random times: (a) displaying a circular pattern; (b) with a hexagonal appearance, especially in the second ring.

to Fig. 3, the average is thus confined to those particles lying within the first-neighbor shell of one of the two particles. An order parameter of zero corresponds to the case where there is no preferred orientation of the particle within the first-neighbor shell, and an order parameter of one corresponds to the case where all particles make a bond angle of exactly $\pi/3$ or $-\pi/3$. The order parameter varies from 0.5 in the solid (at $\rho=1.05$ and $T=1$) to zero at about $\frac{7}{10}$ of the freezing density. The natural logarithm of ζ versus density is plotted in Fig. 5 for the 896-particle system at all densities including a point in the solid, and for the 3584 particle liquid at $\rho=0.9238$. An autocorrelation function $C_\zeta(t)$, was defined as $\langle [\zeta(0)-\zeta][\zeta(t)-\zeta] \rangle$ and normalized to unity at zero time. Figure 6 shows plots of $C_\zeta(t)$ for four densities: $\rho=0.98, 0.95, 0.90,$ and 0.75 . Defining a relaxation time as the half-life of the correlation function, we estimate this time to be 0.15 at $\rho=0.95$, for example. The time falls sharply with density, as is evident from the figure. In general the relaxation time agrees closely with the corresponding Maxwell relaxation time (the ratio of the shear viscosity to the shear modulus).

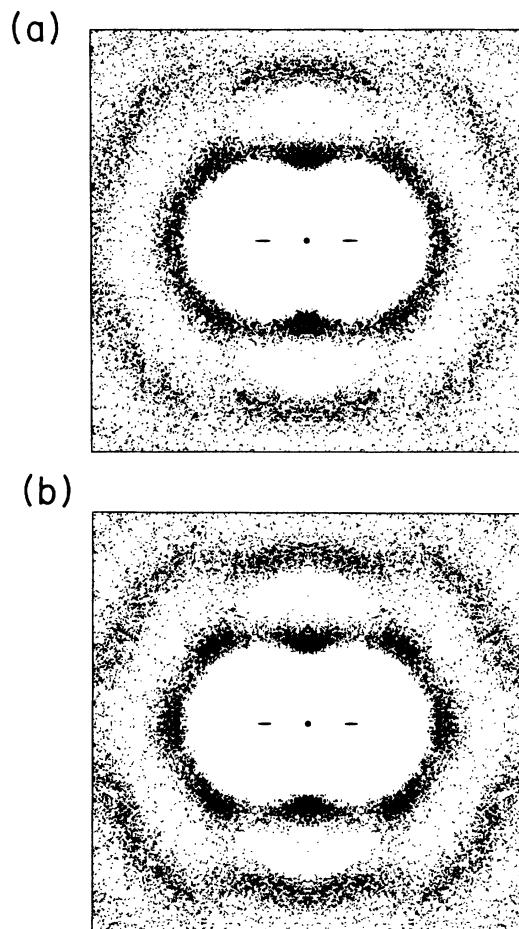


FIG. 3. Frequency plots of the particle positions around the midpoint of the vector connecting a given particle and its nearest neighbor for the liquid at $\rho=0.95$ evaluated from the simulations that were used to obtain $S(\mathbf{k})$ in Fig. 2. (a) corresponds to Fig. 2(a) and (b) to Fig. 2 (b). Note the frequency variation in both bands.

REMARKS AND CONCLUSIONS

We conclude with three remarks.

(1) The order could well be related to the observation that the density dependence of many thermophysical properties of real liquid show a marked change at about $\frac{7}{10}$ of the freezing density—the density at which the order parameter becomes measurable. This change is particularly noticeable for the shear viscosity coefficient¹³ which increases strongly with density, and the diffusion coefficient which has a corresponding decrease with density.^{1,5}

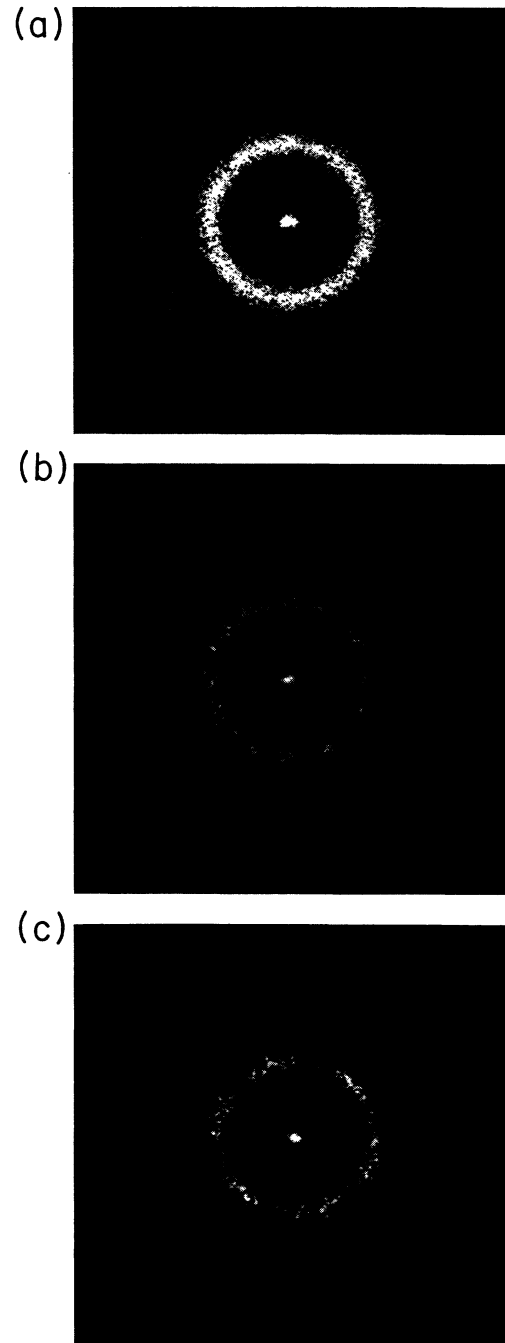


FIG. 4. Structure factor for the 3584-particle liquid at $\rho=0.9238$. (a) displays the $S(\mathbf{k})$ from exposing the whole sample, (b) from various segments of area.

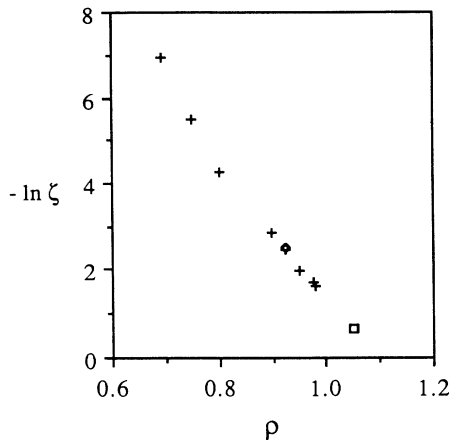


FIG. 5. Plot of $-\ln \zeta$ vs density including that of the solid (square). The value at $\rho=0.9238$ for the 3584-particle system (filled diamond) is essentially superimposed on its equivalent from the 896-particle system. The parameter goes effectively to zero for $\rho < 0.7$.

(2) The work has strong points of similarity with a recent investigation of a real two-dimensional colloidal liquid.¹⁴ Reference 14 reports that an aqueous colloidal suspension at a nominal liquid density was constrained between two flat plates and a laser light Debye-Scherrer pattern observed as a function of plate separation; at a separation of the order of the Debye-Scherrer ring width an observer could see the appearance and disappearance of a six-spot pattern similar to that from the crystalline phase.^{14,15} The fluctuating patterns appeared at random orientation and lasted for tens of milliseconds. Furthermore, the Maxwell relaxation time for the colloidal suspension is of the order of tens of milliseconds. Hence our simulated liquid and the suspension are under equivalent experimental conditions by this criterion. (We make use of this equivalence in a previous study of a model liquid under shear.^{11,2})

(3) Our method probes the equilibrium liquid away from the freezing transition and thus has a different emphasis from complimentary investigations on supercooling and metastability, nevertheless the method is well-suited to such studies. In fact we investigated briefly how

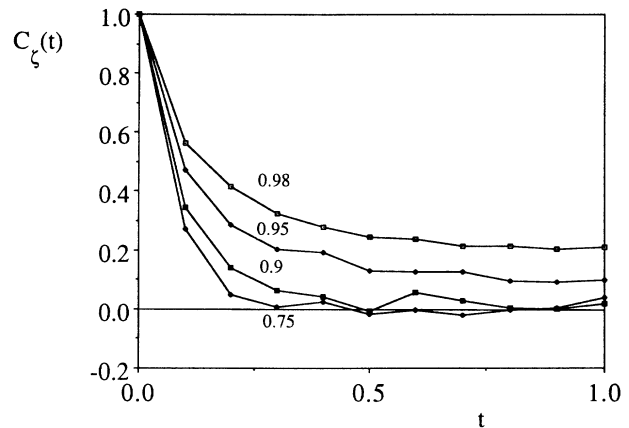


FIG. 6. Plot of $C_\zeta(t)$ vs time at four representative densities: $\rho=0.98, 0.95, 0.90,$ and 0.75 .

ζ and $C_\zeta(t)$ depended on the initial conditions of the simulation at densities close to melting and freezing. As an example, the curve for $\rho=0.98$ in Fig. 6 was evaluated after equilibration from a previous simulation at $\rho=0.975$. The equivalent curve after apparent equilibration from the solid gave quite a different appearance, with an initial decay to $t=0.1$, $C_\zeta(t)$ increased and then became essentially constant. This behavior was consistent with the metastability reported in Ref. 9.

In summary, the existence of transient anisotropy or local order in the liquid has been demonstrated, but it should be stressed that the order reported here does not represent a separate phase of matter characterized by long-ranged long-lived hexagonal bond ordering,¹⁶ but represents fluctuations in the normal liquid phase at high density.¹⁷ The density range over which the structure can be detected by means of an order parameter is large and extends to well below the freezing density.

ACKNOWLEDGMENTS

This work was supported in part by the Office of Engineering and Geothermal Sciences, U.S. Department of Energy. H. Hanley is most grateful for the hospitality of the Staff of the Research School of Chemistry, the Australian National University.

*Permanent address: Thermophysics Division, National Bureau of Standards, Boulder, CO 80303.

¹For example, C. A. Angell, J. H. R. Clarke, and L. V. Woodcock, *Adv. Chem. Phys.* **48**, 397 (1981).

²D. Frenkel and J. P. McTague, *Ann. Rev. Phys. Chem.* **31**, 491 (1980).

³C. S. Hsu and A. Rahman, *J. Chem. Phys.* **70**, 5234 (1979); **71**, 4974 (1979).

⁴R. D. Mountain, *Phys. Rev. A* **26**, 2859 (1982).

⁵J. R. Fox and H. C. Andersen, *J. Phys. Chem.* **88**, 4019 (1984).

⁶S. Hess, *J. Phys. (Paris), Colloq.* **46**, C3-191 (1985).

⁷D. J. Evans and G. P. Morriss, *Comp. Phys. Rep.* **1**, 297 (1984).

⁸For example, D. J. Evans, and G. P. Morriss, *Phys. Rev. Lett.* **51**, 1776 (1983); L. V. Woodcock, *Chem. Phys. Lett.* **111**, 455 (1984).

⁹D. J. Evans, *Phys. Lett.* **88A**, 48 (1982).

¹⁰G. Harburn, C. A. Taylor, and T. R. Welberry, *An Atlas of Optical Transforms* (Bell, London, 1975).

¹¹H. J. M. Hanley, G. P. Morriss, T. R. Welberry, and D. J. Evans, *Physica A* **149**, 406 (1988).

¹²H. J. M. Hanley, J. C. Rainwater, N. A. Clark, and B. J. Ackerson, *J. Chem. Phys.* **79**, 4448 (1983).

¹³D. E. Diller and L. J. Van Poolen, *Int. J. Thermophys.* **6**, 43 (1985).

¹⁴N. A. Clark, B. J. Ackerson, and A. J. Hurd, *Phys. Rev. Lett.* **50**, 1459 (1983); N. A. Clark, B. J. Ackerson and T. W. Taylor, *J. Phys. (Paris) Colloq.* **46**, C3-137 (1985).

¹⁵N. A. Clark (private communication).

¹⁶B. I. Halperin and D. R. Nelson, *Phys. Rev. Lett.* **41**, 121 (1981).

¹⁷F. H. Stillinger and T. A. Weber, *Phys. Rev. A* **25**, 978 (1982).

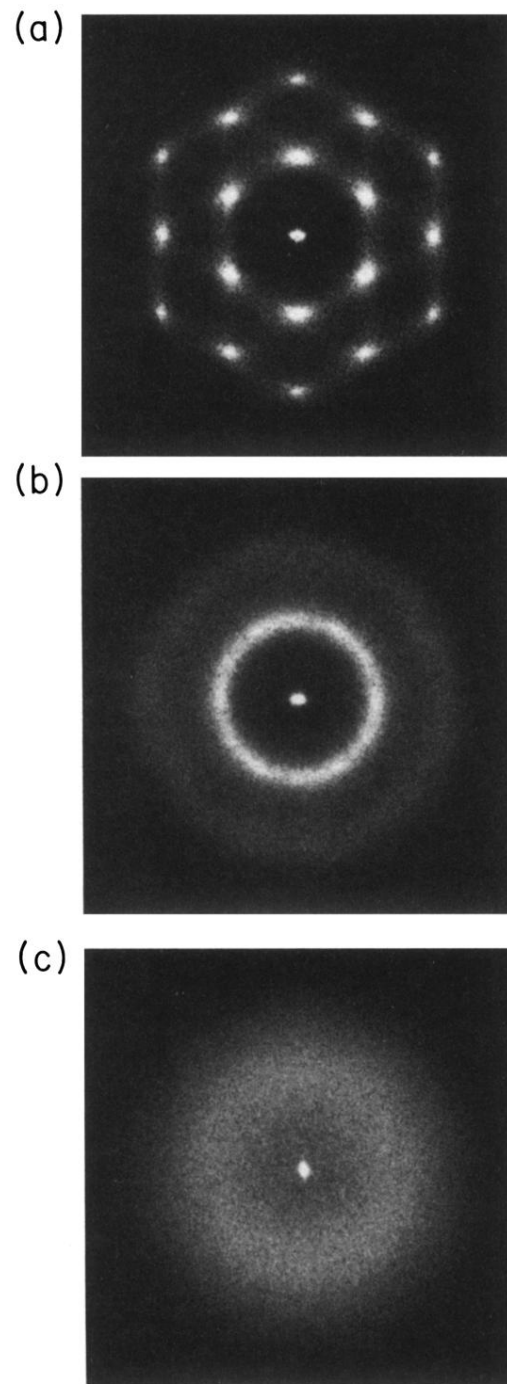


FIG. 1. Average structure factors for the 896-particle soft-disk system at three densities. (a) The solid at $\rho=1.05$; (b) dense liquid at $\rho=0.95$; (c) the liquid at $\rho=0.3$.

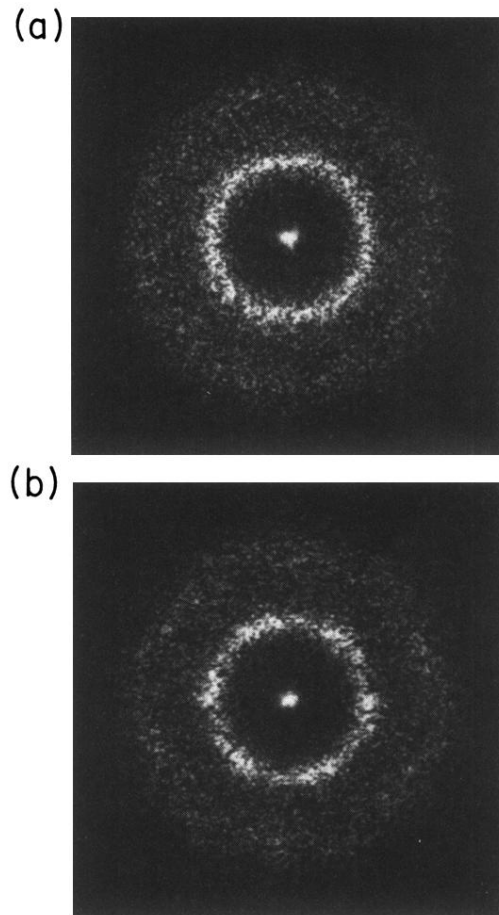


FIG. 2. The structure factor for the liquid at $\rho=0.95$ evaluated from the simulation at two random times: (a) displaying a circular pattern; (b) with an hexagonal appearance, especially in the second ring.

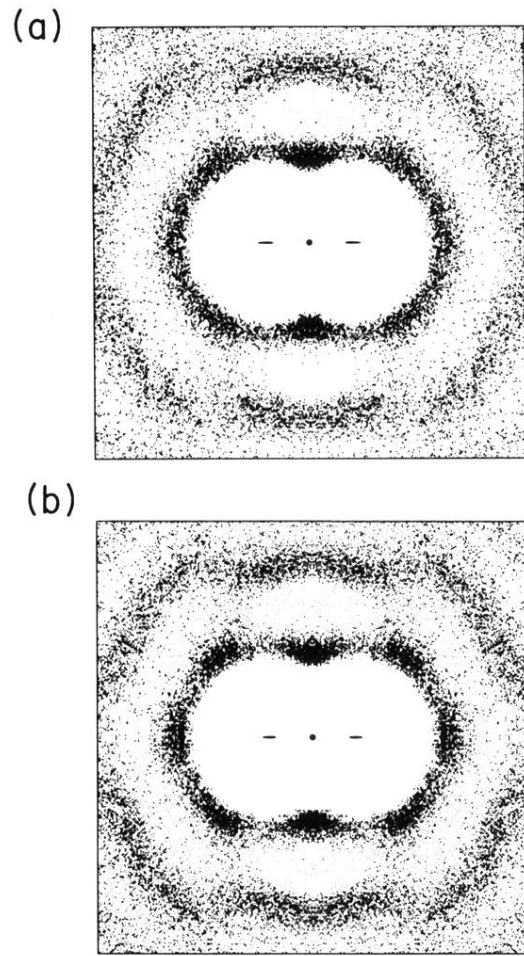


FIG. 3. Frequency plots of the particle positions around the midpoint of the vector connecting a given particle and its nearest neighbor for the liquid at $\rho=0.95$ evaluated from the simulations that were used to obtain $S(\mathbf{k})$ in Fig. 2. (a) corresponds to Fig. 2(a) and (b) to Fig. 2 (b). Note the frequency variation in both bands.

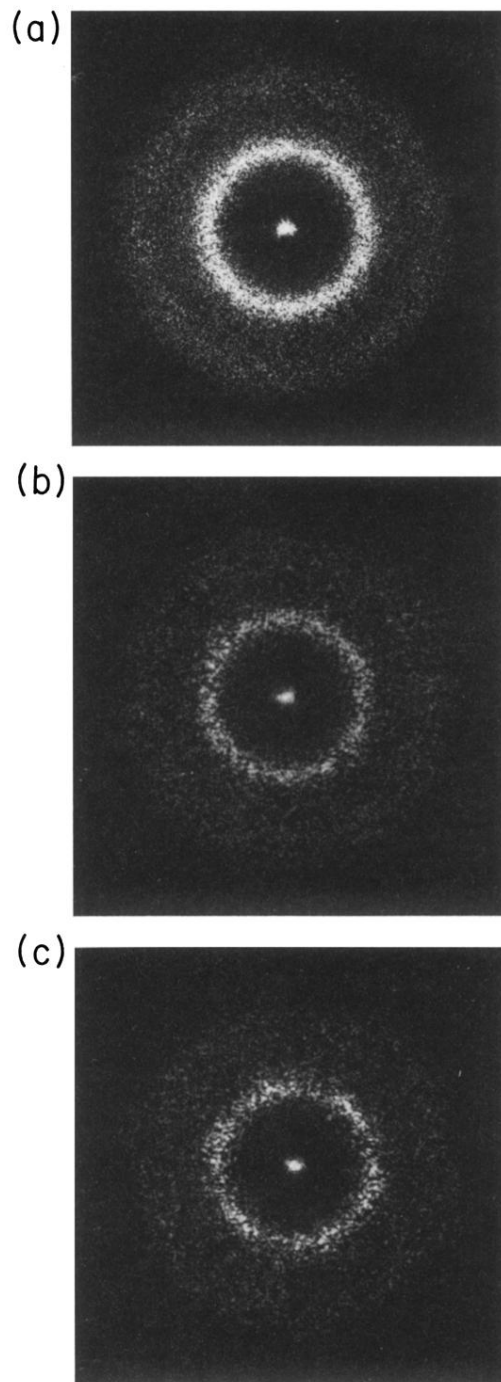


FIG. 4. Structure factor for the 3584-particle liquid at $\rho=0.9238$. (a) displays the $S(\mathbf{k})$ from exposing the whole sample, (b) from various segments of area.